Technical Validation of the RLS Smart Grid Approach to Increase Power Grid Capacity without Physical Grid Expansion

Ramón Christen[1], Vincent Layec[2], Gwendolin Wilke[1] and Holger Wache[2]
[1]*Department of Computer Science, University of Applied Science Lucerne, Rotkreuz, Switzerland*
[2]*Institute of Information Systems, University of Applied Science and Arts of Northwestern Switzerland, Olten, Switzerland*

Keywords: Smart Grid, Power Grid, Grid Capacity, Grid Reinforcement, Load Prediction, Load Management.

Abstract: The electrification of the global energy system and the shift towards distributed power production from sustainable sources triggers an increased network capacity demand at times of high production or consumption. Existing energy management solutions can help mitigate resulting high costs of large-scale physical grid reinforcement, but often interfere in customer processes or restrict free access to the energy market. In a preceding paper, we proposed the RLS regional load shaping approach as a novel business model and load management solution in middle voltage grid to resolve this dilemma: market-based incentives for all stakeholders are provided to allow for flexible loads that are non-critical in customer processes to be allocated to the unused grid capacity traditionally reserved for N-1 security of supply. We provide a validation of the technical aspects of the approach, with an evaluation of the day-ahead load forecasting method for industry customers and a load optimization heuristics. The latter is tested by a simulation run on a scenario of network branch with provoked capacity bottlenecks. The method handles all provoked critical network capacity situations as expected.

1 INTRODUCTION

With the ongoing change away from fossil resources toward electric power, an increase in electric power demand and in production and consumption concurrency can be foreseen. As a result, higher grid capacities are required to avoid grid congestion. To help mitigate the high costs of assumed future large scale physical grid expansions, IT-based energy management solutions in the ”Smart Grid” have been proposed for a more efficient use of existing capacities (Atzeni, 2014). Yet, most of these grid-optimizing approaches interfere with customer processes and do not rely on market-based principles. In contrast, market-based energy management approaches usually disregard the perspective of grid optimization.

In (Bagemihl et al., 2018), a business model has been proposed that provides market-based incentives to all stakeholders on the medium voltage grid levels to utilize so-called ”conditional” flexible loads for grid capacity optimization. The business model is associated with a load management approach for ”Regional Load Shaping” (RLS) with a day-ahead optimization heuristics that considers both, customer-side energy prizes and grid capacity constraints of network branches, at the same time. In order to allow for grid capacity increase without necessitating physical grid expansion, the RLS approach proposes to allocate for so-called ”conditional loads” the currently unused grid capacity dedicated to ensuring the (n-1) security of supply. That capacity is reserved for the case of rare grid disturbance where one branch takes over the loads of another branch. I.e., conditional loads comprise flexibilities that may be temporarily shedded in the event of grid disturbance. They contrast with ”unconditional loads”, which require security of supply all-time, such as, loads required for industrial production processes.

In the present paper, we test and validate the technical aspects of the RLS approach, namely the RLS optimization heuristics and the underlying day-ahead load forecasting method. For testing and validation we simulate network congestions by extrapolating a real world scenario of our pilot customers to future scenarios with increased power demand and supply. We show that the proposed load scheduling solution with its prize optimization heuristics handles the critical network capacity situations as expected. For the evaluation of the day-ahead load forecasting method, we evaluate the Mean Absolute Percentage Error (MAPE) as a measure of accuracy and show that the results achieved with our pilot customers’

Christen, R., Layec, V., Wilke, G. and Wache, H.
Technical Validation of the RLS Smart Grid Approach to Increase Power Grid Capacity without Physical Grid Expansion.
DOI: 10.5220/0007717101230130
In *Proceedings of the 8th International Conference on Smart Cities and Green ICT Systems (SMARTGREENS 2019)*, pages 123-130
ISBN: 978-989-758-373-5

data sets are comparable with results in the literature. Additionally, we evaluate the prediction reliability as a means for the Distribution System Operator (DSO) and end customer to assess the prediction quality from a pragmatic perspective.

2 STATE OF THE ART

2.1 Load Scheduling Approaches

Shifting the electrical consumption to another time is a Demand Response (DR) case, a change in electric usage by prosumer (household or industrial customer) from its normal demand pattern in reaction to an incentive payment. The review of (Shariatzadeh et al., 2015) distinguished dispatchable programs where the prosumers let the DSO control their systems from non-dispatchable programs where the prosumers decentrally set their load schedule. The latter category spans from simple Time-Of-Use (TOU) with constant day and night prices to Real-Time Pricing (RTP), a tariff changing at each time step. In (Doostizadeh and Ghasemi, 2012), the information about the price is communicated one day in advance so prosumers do not need to predict prices. But automatic schedulers participating with the same information will plan their load in the same cheapest timestep and unfortunately create new peaks (Zhao et al., 2013). The formulation of the schedulers (mathematical programming, metaheuristics or other controllers) depends on the type of tariff system, but also on the type of electrical loads, their operating constraints, the number of timesteps, the type of variables (without integer or not), as classified in (Shaikh et al., 2014). The case of photovoltaic in combination with several battery types is addressed in (Thirugnanam et al., 2018). The issue of synchronisation is tackled in (Mohsenian-Rad and Leon-Garcia, 2010) with tariff of Inclining Block Rates (IBR) where high consumption levels are dissuasively expensive. (Hunziker et al., 2018) showed that the total load of a community of prosumers can be well shaped with tariffs combining RTP with IBR. So far, no tariff system targets the paradox that in grids half of the transmission capacity is reserved as a redundancy for the rare case of failure and remains an expensive unused resource.

2.2 Prediction Methods for Day-ahead Forecasting for Industry Customers

A growing importance of efficient energy usage and an even more decentralized sustainable power production increases the focus in research on prediction of time series for power demand. In that field, James W. Taylor has done several works in time series prediction such as (Taylor et al., 2006; Taylor et al., 2007; Taylor, 2010). A major differentiation in research is done in the aggregation level of the predicted power demand. Commonly it is said, the higher the level the less the prediction accuracy. This behavior is shown in several papers (Zufferey et al., 2016; Arora and Taylor, 2016; Mirowski et al., 2014). A comparison of the aggregation level versus the prediction accuracy in (Mirowski et al., 2014) confirms this dependency. A similar behaviour is also shown by Kong *et. al* that predicted individual residential power demand with a Long Short-Term Memory (LSTM) network and a precision of a MAPE of approx. 44% compared to an aggregate forecast with a MAPE of approx. 8% (Kong et al., 2017). The strength of a LSTM network for an electrical load forecast compared to other common methods such as Support Vector Regression (SVR) are shown in (Zheng et al., 2017) with an achieved MAPE of less than 6%.

Further, for a prediction also the usage of power is differentiated, i.e. whether the time series is of a residential or an industrial consumption. In (Kong et al., 2017) it is mentioned that industrial electricity consumption patterns would be more regular than residential ones such that Ryu *et al.* achieved in (Ryu et al., 2016) a prediction accuracy for industrial loads with a MAPE of about 8.85%. Less accurate predictions were obtained in (Ghofrani et al., 2011) for residential loads by means of a Kalman filter estimator. Mocanu *et. al* presented in (Mocanu et al., 2016) different deep learning approaches whereas the implementation of a Factored Conditional Restricted Bolzman Machine (FCRBM) outperformed several Machine Learning (ML) algorithms.Comparable results were achieved by Marino *et. al* by using a LSTM network (Marino et al., 2016) and Shi for household load forecasting (Shi et al., 2018).

3 THE RLS APPROACH

3.1 Increasing Grid Capacity

In most grids system availability must be guaranteed in case of failure of a single network component such as, e.g., a power line or transformer unit. As a result a percentage of the grid capacity is not used in normal operation, but reserved for this so-called (N-1) security of supply. However, the large majority of days go without grid failure.

The RLS approach proposes to allocate the normally unused grid capacity reserved for (N-1) secu-

rity of supply to conditional loads. Here, *conditional loads* are loads for which (1) (N-1) security of supply is not essential, (2) that are highly price-sensitive, and (3) that are flexible and may thus be used for price optimization purposes via load management. Conditional loads comprise, e.g., the charging of stationary batteries for internal consumption or power heat coupling for fuel substitution. *Unconditional loads* are all other loads.

Since security of supply is by definition not essential for conditional loads this unused grid capacity may be dedicated to them without compromising the important security of supply level for conventional household and industrial loads: in case of a branch failure, conditional loads are shedded to provide security for unconditional loads.

Figure 1 illustrates a simplified version of the used and unused grid capacity. Here, the component's maximal capacity is split exemplarily in two capacity bands of 50% each. The lower band shown in blue is the capacity used in normal operation, while the upper band shown in grey represents the unused capacity reserved for security. We call this band the *N-1 band* because it ensures N-1 security to another branch. Notice that the width of the N-1 band of a network branch is determined by the component with smallest capacity. The day-ahead prediction of unconditional loads (dark blue) and the scheduling of conditional loads (green) is the subject of the rest of this paper.

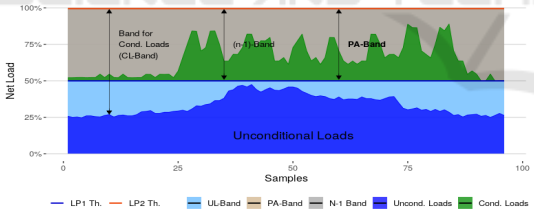

Figure 1: Example of a load schedule split in unconditional loads (blue) and conditional loads (green).

In the RLS approach, the market-based *incentive for customers* to register some of their flexibilities as conditional loads is (1.) a load schedule management for energy price optimization and (2.) a significantly lower grid fee compared to unconditional loads. *Incentives for distribution system operators (DSO)* to implement the RLS approach comprise (1.) the possibility to postpone or avoid large scale physical grid expansion, (2.) achieving a small increase in income by additionally charged grid costs for the N-1 band, and (3.) higher transparency within the grid due to customer side load measurement and DSO-registered load schedules.

3.2 Scheduling Conditional Loads

The goal of the day-ahead scheduling of conditional loads is to minimize energy prizes for all customers connected to the network branch under consideration. The minimization is subject to (1.) the customers' chosen prizing models, (2.) to their operating constraints (dependent on the flexible loads in use), and (3.) to given grid constraints. Since regulations require that grid control and provision of energy supply must be operated by separate legal entities, the management software is split in two independent subsystems: the *Grid Manager (GM)* is operated by the DSO and monitors grid constraints; the *Energy Manager (EM)* implements the customer perspective and collects the individually price-optimized load schedules of all connected customers and aggregates them. An iterative optimization heuristics implements the interaction of GM and EM in order to ensure grid and customer constraints. Each iteration comprises two steps:

1. *Local optimization:* The EM calculates a price-optimized conditional load schedule for a participating customer, which (if given) respects the grid constraints prescribed by step 2. It submits the schedule to the GM.
2. *Global optimization:* The GM aggregates the accumulated loads from different customers and checks grid capacity constraints. In case the N-1 band capacity is exceeded, the GM curtails each customer's schedule according to their chosen prizing model and submits to the EM an adapted schedule based on load optimization on the aggregated level; they then can optimise theri schedule again (step 1).

The process is reiterated until a predefined time-based deadline is reached and final schedules of the next day are sent to the controllers of each customer's devices.

In step one, each customer initially submits his desired schedule of conditional loads for the next day to the GM, i.e. a time series of the power of each aggregate a for each timestep t. It is computed by solving a minimization of the daily energy costs subject to operations constraints of conditional loads, such as the energy balance for battery. Costs of substituted fossil fuels and costs of electricity - via the actual power and the actual electricity price - are considered. The actual power is the net power supplied by the grid, so the sum of unconditional resp. conditional loads, corrected by the own photovoltaic (PV) production. The electricity price is made of a spot price timeserie predicted for year 2035 plus other fees *OF* (grid, taxes and duties). For unconditional loads in the so-called Standard Tariff (STT), *OF* is assumed to grow up to 10 ct. / kWh until 2035. We introduce

a so-called Power Alliance Tariff (PAT) with reduced *OF* of only 4.8 ct / kWh in order to give a financial incentive to use conditional loads. *OF* is 0 ct / kWh when the power is fed back to the grid, so that the use of own overproduction of PV remains the cheapest option to schedule conditional loads, whereas importing power at PA Tariff during timesteps of low spot price becomes the second cheapest option.

In step two, initially submitted schedules are aggregated, controlled and adjusted by the GM. On the time steps with synchronized original loads exceeding the grid limit, a centralized algorithm computes an allocation respecting them with consideration of the load asked by each customer *c* and their financial participation of this system of conditional loads. Once completed, a decentralized algorithm allocates loads at customer level for each of the aggregates.

3.3 Day-ahead Load Forecasting

The second technical aspect of the RLS approach evaluated in the paper is the day-ahead prediction of the unconditional loads of industry customers. It serves two purposes: (1.) to provide customers with higher transparency and thus better control of their energy usage - it thereby serves as an additional incentive to participate in the program; (2.) to allow for optimized usage of the currently unused grid capacity in future scenarios.

For the day-ahead load forecasting of customer load profiles, a *model selection approach (MSA)* has been chosen. Thereby, a set of different time series forecasting models are trained, fitted and evaluated based on historical load profile data that comprises 14, 28, 42, 56 and 70 days for every individual customer. The best model and training data length is chosen separately for each customer based on the MAPE performance evaluation metric. The MSA is executed in regular time intervals (e.g. every month) in order to allow for continuous adaptations to changes in the customer load profile characteristics.

16 different prediction models where included: As a *benchmark model*, the load profile of the previous workday / non-working day was used as forecast for the following day, respectively. The *similar days model* was included in three variants: SD1 uses the median of a set of historical days of the same weekday (e.g., the five previous Mondays) as a forecast, SD2 uses the median of a set of previous workdays or non-working days, respectively, and SDEns takes the median of the forecasts of SD1 and SD2. The classical time series prediction models *Exponential Smoothing (ES)*, *Random Walk Drift (RWD)*, *Hold Winters (HW)*, *Auto-Regressive Integrated Moving Average (ARIMA)* and *Generalized Autoregressive Conditional Heteroskedasticity (GARCH)* each where applied both directly to the original load profile and to the residual of the load profile after decomposition. The latter version is referred to with the add on *Dec* after the model name: *ES Dec*, *RWD Dec*, *HW Dec*, *ARIMA Dec*, and *GARCH Dec*. Finally, a support vector machine with a radial bias kernel was applied in both variants, *SVR* and *SVR Dec*.

4 SCHEDULING VERIFICATION

In order to test the scheduling approach for conditional loads, we provoke a grid congestion in a scenario based on real data of three pilot customers A, B and C and one ad-hoc customer X.

4.1 Settings of the Experiment

Present energy usage of customers A, B and C are classified in Table 1 in thermal or non thermal usage. Photovoltaic panels will be installed on their roofs. A new customer X, representative for several new customers like freight shipping companies with new Power-To-Gas units up to 7 MW but without significant own compulsory loads nor PV, is added to simulate a congestion of the band of conditional loads. No other grid related carrier (district heating) or off grid (heating oil, pellets, etc.) is considered here. New units of Table 2 are assumed to be added. "Other" aggregates of C (a food industry) are hereby cooling machines using the frozen food as thermal storage and substituting electricity of a cooling machine of a later timestep of the same day.

Table 1: Energy carrier and usage (kW peak) of customers.

usage	electric cooling	electric process	process with gas	heat from gas
A	700	1000	-	500
B	-	300	-	200
C	2000	1700	1000	1000

Table 2: Assumed new conditional loads and PV (kW).

	P-to-Heat	P-to-Gas	Battery	other	PV
A	500	-	-	-	1500
B	-	300	100	-	900
C	-	-	-	2x250	1900
X	-	7000	-	-	-

A fictive grid configuration with all customers A, B, C and X in the same branch is assumed to evaluate our method. Each power line (asset) has here a capacity of 12 MW and is not used over 6 MW to provide reserve capacity. In the first asset of the branch, compulsory loads reaches today 5.4 MW (no bottleneck).

With the new loads, the sum grows to 13.8 MW (bottleneck). Moreover, simultaneous conditional loads can reach 8.4 MW and thus exceed the capacity of 6 MW of the N-1 band.

4.2 Initially Submitted Schedules

Figure 2 with power on left y-axis against time on x-axis shows the initial solution (i.e. before control of grid limits) of the load scheduling problem for customers A (top row), B (middle row) and X (bottom row) for the cloudy winter day of January, 11th. Consumption respectively production are displayed separately on the left resp. right graph. Grey bands represent the split in Standard Tariff for compulsory loads in the lower part of positive power and Power Alliance Tariff in the upper part with conditional load. Negative power is fed back to the grid. In customer A, the PV unit (yellow) substitutes part of electricity import from grid (black), and is used to run the power-to-heat unit (blue) to substitute natural gas. The P-t-H unit will also run with the cheap electricity price of PAT (black, brindled) during afternoon hours with the lowest spot price of the day. The Power-to-Gas units of Customer X, as well as the Power-to-Gas unit (blue) and the charging (red) of battery of Customer B will run at the same afternoon hours as customer A due to the spot price. Discharging (green) happens here in morning hours, before charging, either for substituting import from grid (black) or for feed back to grid (purple), with a sufficient battery capacity assumed in this model. The cooling units of Customer C (not displayed) are modelled like a battery but with the hygiene constraint that charging can only precede discharging, as the storage medium is the frozen food. Therefore they run in the morning at a different timestep than A and B.

4.3 Curtailment in Case of Excess Load

On Grid Level: GM controls the cumulative load of all customers, displayed in Figure 3 with compulsory resp. conditional loads in the lower resp. upper part. When the lowest electricity spot price is attained between 2 p.m. and 6 p.m., conditional loads from A, B and X get aggregated with 7.9 MW (left graph). The conditional loads exceed the grid capacity limit of 6 MW of the N-1 band and should be reduced by 1.9 MW. The loads are re-allocated for all customers A, B and X according to a rationing scheme of Table 3. The curtailment is done proportionally to the number of points (allowances) of each customer without exceeding their initially submitted schedule. In case a customer asked less than its allowance (here C), the remaining non-allocated capacity is redistributed iteratively among the other customers to avoid waste of capacity.

Table 3: Curtailment on grid level.

	points	submitted (kW)	final (kW)
A	500	500	379.7
B	400	400	303.8
C	500	0	0
X	7000	7000	5316.5
sum	8400	7900	6000

On Aggregate Level: After each customer reads the amount of its curtailment for each timestep, it computes the local curtailment on the level of each aggregate. Aggregates are modelled here with an integer number of stages between a minimal (here 0) and maximal power. The allocation with least wasted capacity is solved as a subsum problem. Table 4 shows the local curtailment of timestep 53 of customer B. Both units are cut in order to reach 303 kW, the maximal value not exceeding the allowance of 303.8 kW from Table 3. The cases of Customer A (with only one unit of P-to-H) and of Customer X (with four units of P-to-G) are treated in a similar way. The schedule of "discharging" is finally adjusted on customers with battery like B to respect the daily energy balance.

Table 4: Curtailment on aggregate level for customer B.

	max	levels	original (kW)	final (kW)
P-to-G	300	100	300	204
charging	100	100	100	99
sum	400	-	400	303

4.4 Discussion

With new loads, two issues were expected: (1.) In the absence of the concept of conditional loads, a grid reinforcement would have been needed in the first asset (even with only the new loads of customers A, B and C). (2.) in presence of customer X and due to load synchronization at the cheapest timestep, the 6 MW of N-1 band were overbooked in the initial schedules and a reinforcement would have been needed in absence of curtailment. The RLS approach with use of N-1 band and with curtailments solves both problems and enables finding schedules valid for both sides. The schedule curtailed by GM fulfills the grid limit without wasting of capacity in the N-1 band. EM reduces schedules on aggregate level accordingly without neither wasting capacity nor disturbing the energy balance of batteries. In the aggregated schedule in Figure 3, the effective use of the N-1 band drops from 26.7 % (left) to only 22.0 % (right, after curtailment) but the system is safe for all stakeholders to be operated.

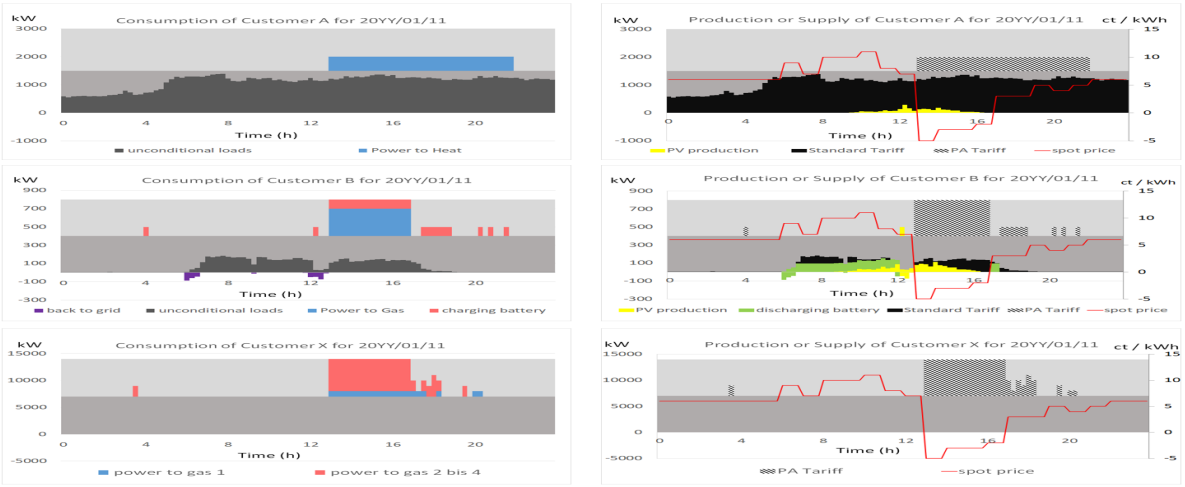

Figure 2: Initial solution of schedule for customers A (top), B (middle) and X (bottom).

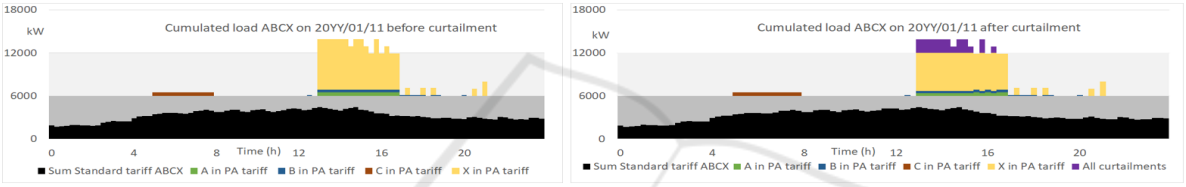

Figure 3: Cumulated load of Customers A, B, C and X in the first asset of the grid branch: initial (left) and curtailed (right).

5 LOAD FORECASTING

5.1 Underlying Data Set

Our test data set comprises 34 end node load profiles of 31 customer including three pilot customers. All of them have a minimum yearly power demand of 200kW. Time series that were available for multiple years have been split into separate fictitious end nodes such that finally time series of 40 end nodes were available for one full year. Applied pre-processing steps as down- and up-sampling, replacement of missing data points, time shifts to match summer and winter time as well as leap years ensure the comparability between all time series.

5.2 Evaluation of Prediction Accuracy

We use the MAPE as a metric for evaluating the prediction accuracy of our test data set. Figure 4 summarizes the results. Here, the employed models are indicated on the horizontal axes and ordered by increasing complexity, on the y-axes the average MAPE is shown when a model is applied in a one-fits-all manner to all end-nodes. The black horizontal line indicates the average MAPE of the MSA with 22.6% (averaged over all end-nodes). This result is competitive with results in literature in comparable settings (Marino et al., 2016; Shi et al., 2018). A single model yields a considerable higher average MAPE than the MSA. Yet, when compared to the SD1 model with an average MAPE of 25.6%, the MSA does not achieve considerably higher prediction accuracy on average. This result suggests that the much higher computational effort of employing the MSA does not justify the relatively small gain in prediction accuracy when employing the very simple SD1 model.

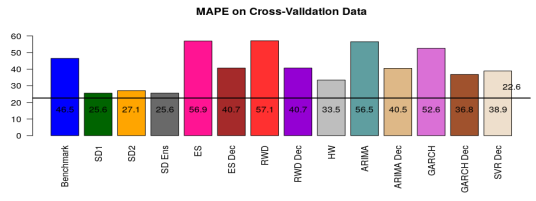

Figure 4: Overview of prediction accuracy of all integrated algorithms in the Model Selection Approach (MSA).

In order to analyze this result in more detail, we compared the prediction accuracy of the MSA with the prediction accuracy of the SD1 model for each single end-node. The distribution of the differences $MAPE(SD1) - MAPE(MSA)$ shows that no accuracy gain is provided by the MSA for 10 of the 40 end

nodes. In other words, for 25% of the end-nodes, the best performing model selected by the MSA is the SD1 model itself. Yet, it also showed that the MSA achieves a MAPE increase of more than 25.6% for 14 of the 40 end-nodes. This amounts to an accuracy improvement of more than 100% when compared to SD1. Particularly, for two end-nodes, the MSA achieves a MAPE increase of about 140% and 200%, respectively. That means while the MSA does not provide considerable improvement of prediction accuracy on average, it does improve the prediction accuracy for some single end-nodes dramatically.

Furthermore, figure 4 shows that for our test data on average simpler models tend to achieve better results than more complex ones. This result is consistent with the experience of our partner DSOs.

5.3 Evaluation of Prediction Reliability

The MAPE as a measure of prediction *accuracy* does not provide end-customers and DSOs with a measure of prediction *reliability* (i.e., accuracy *and* precision). Yet, a reliable day-ahead prediction of load demands is pivotal since it increases their ability to plan and decreases financial risk considerably. Prediction intervals as measures of prediction reliability rely on the assumption of normally distributed errors, an assumption that is violated for most of our test data. While it is usually possible to find suitable transformations for single load profiles manually, automating this process as a part of the RLS software is not a straight forward task. Hence, we assessed the ”true” reliability of prediction intervals based on historic data.

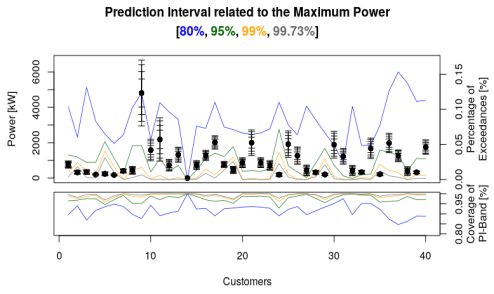

Figure 5: Historic prediction reliability per end node.

The lower part of figure 5 shows the historic prediction reliability for our test data: for each of the 40 end nodes the percentage of observations falling in the 80%, 95%, 99% and 99.73% prediction interval (PI) is shown in the figure as a blue, green, yellow and grey line plot, respectively. It can be seen that the historic reliability of the 99% and 99.73% PI is greater than 95% for all end nodes. The upper part shows the inverse percentage (i.e., the percentage of observations exceeding the upper limits of the respective PIs), together with error bars indicating the PI.

5.4 Discussion

Two main findings are discussed. (1.) While the MSA only achieves a negligible increase of 3% in MAPE on average compared to the simplistic SD1 model, it allows an accuracy increase of more than 25% for 35% of the end nodes and a dramatic increase of over 100% in MAPE for two end nodes. The result justifies the drastically higher computational effort in employing an MSA compared to SD1. In operation, excluding never chosen models from the MSA will increase the computational efficiency. Yet, to accommodate possible changes in the data sources, they are included in every n-th model training/fitting iteration step. To further improve prediction accuracy, LSTM neural networks are tested for selected customers with additional customer-specific information. (2.) With a true reliability of 95%, tests on the prediction reliability - measured by the true percentage of observations falling in the 99% prediction interval - have been satisfactory, and serve to assess the usefulness of predictions as a day-ahead load schedule for unconditional loads within the RLS context. Here, the upper band of the prediction interval determines the margin of unused grid capacity that may be used to further optimize the scheduling of conditional loads.

6 CONCLUSIONS

We tested and validated the technical aspects of the RLS approach currently deployed at the pilot customers with live data and comprising (1.) grid-aware load scheduling with heuristic price optimization, and (2.) day-ahead prediction of individual unconditional customer loads. Thanks to the control of grid limits by the DSO and subsequent curtailment, the load scheduling method is safe for use even if the amount of initially submitted conditional loads exceeds the N-1 band. The functionality of the system is verified. Planned improvements include an analysis of the fairness, efficiency and performance of the curtailment mechanisms with the goal to further decrease energy costs. The evaluation of the model selection approach for predicting unconditional loads w.r.t. accuracy and reliability showed competitive results with the literature. Future work include an extension of the load scheduling approach with the goal to use the full range of unused grid capacity for future congestion scenarios. To this end the band used for load shifting will be extended from the fixed-width N-1 band to the

variable-width CL-band (cf. figure 1). It is bounded by the upper limit of the PI of the day-ahead prediction of uncond. loads used as day-ahead schedule.

REFERENCES

Arora, S. and Taylor, J. W. (2016). Forecasting electricity smart meter data using conditional kernel density estimation. *Omega*, 59:47–59.

Atzeni, I. (2014). *Distributed demand-side optimization in the smart grid*. PhD thesis.

Bagemihl, J., Boesner, F., Riesinger, J., Künzli, M., Wilke, G., Binder, G., Wache, H., Laager, D., Breit, J., Wurzinger, M., Zapata, J., Ulli-Beer, S., Layec, V., Stadler, T., and Stabauer, F. (2018). A market-based smart grid approach to increasing power grid capacity without physical grid expansion. *Computer Science - Research and Development*, 33(1-2):177–183.

Doostizadeh, M. and Ghasemi, H. (2012). A day-ahead electricity pricing model based on smart metering and demand-side management. *Energy*, 46:221–230.

Ghofrani, M., Hassanzadeh, M., Etezadi-Amoli, M., and Fadali, M. S. (2011). Smart meter based short-term load forecasting for residential customers. In *2011 North American Power Symposium*, pages 1–5.

Hunziker, C., Schulz, N., and Wache, H. (2018). Shaping aggregated load profiles based on optimized local scheduling of home appliances. *Computer Science - Research and Development*, 33:61–70.

Kong, W., Dong, Z. Y., Jia, Y., Hill, D. J., Xu, Y., and Zhang, Y. (2017). Short-term residential load forecasting based on lstm recurrent neural network. *IEEE Transactions on Smart Grid*.

Marino, D. L., Amarasinghe, K., and Manic, M. (2016). Building energy load forecasting using deep neural networks. In *Industrial Electronics Society, IECON 2016-42nd Annual Conference of the IEEE*, pages 7046–7051. IEEE.

Mirowski, P., Chen, S., Ho, T. K., and Yu, C.-N. (2014). Demand forecasting in smart grids. *Bell Labs technical journal*, 18(4):135–158.

Mocanu, E., Nguyen, P. H., Gibescu, M., and Kling, W. L. (2016). Deep learning for estimating building energy consumption. *Sustainable Energy, Grids and Networks*, 6:91–99.

Mohsenian-Rad, A.-H. and Leon-Garcia, A. (2010). Optimal residential load control with price prediction in real-time electricity pricing environments. *IEEE Transactions on Smart Grid*, 1:120–133.

Ryu, S., Noh, J., and Kim, H. (2016). Deep neural network based demand side short term load forecasting. *Energies*, 10(1):3.

Shaikh, P. H., Bin Mohd Nor, N., Nallagownden, P., Elamvazuthi, I., and Ibrahim, T. (2014). A review on optimized control systems for building energy and comfort management of smart sustainable buildings. *Renewable and Sustainable Energy Reviews*, 34:409–429.

Shariatzadeh, F., Mandal, P., and Srivastava, A. K. (2015). Demand response for sustainable energy systems: A review, application and implementation strategy. *Renewable and Sustainable Energy Reviews*, 45:343–350.

Shi, H., Xu, M., and Li, R. (2018). Deep learning for household load forecasting—a novel pooling deep rnn. *IEEE Transactions on Smart Grid*, 9(5):5271–5280.

Taylor, J. W. (2010). Triple seasonal methods for short-term electricity demand forecasting. *European Journal of Operational Research*, 204(1):139–152.

Taylor, J. W., De Menezes, L. M., and McSharry, P. E. (2006). A comparison of univariate methods for forecasting electricity demand up to a day ahead. *International Journal of Forecasting*, 22(1):1–16.

Taylor, J. W., McSharry, P. E., et al. (2007). Short-term load forecasting methods: An evaluation based on european data. *IEEE Transactions on Power Systems*, 22(4):2213–2219.

Thirugnanam, K., Kerk, S. K., Yuen, C., Liu, N., and Zhang, M. (2018). Energy management for renewable microgrid in reducing diesel generators usage with multiple types of battery. *IEEE TRANSACTIONS ON INDUSTRIAL ELECTRONICS*, 65:6772–6786.

Zhao, Z., Lee, W., Shin, Y., and Song, K. (2013). An optimal power scheduling method for demand response in home energy management system. *IEEE Transactions on Smart Grid*, 4:1391–1400.

Zheng, J., Xu, C., Zhang, Z., and Li, X. (2017). Electric load forecasting in smart grids using long-short-term-memory based recurrent neural network. In *Information Sciences and Systems (CISS), 2017 51st Annual Conference on*, pages 1–6. IEEE.

Zufferey, T., Ulbig, A., Koch, S., and Hug, G. (2016). Forecasting of smart meter time series based on neural networks. In *International Workshop on Data Analytics for Renewable Energy Integration*, pages 10–21. Springer.